Lattice-Boltzmann method for the simulation of transport phenomena in charged colloids

Jürgen Horbach* and Daan Frenkel
Kruislaan 407, 1098 SJ Amsterdam, The Netherlands
(Received 6 July 2001; published 21 November 2001)

We present a simulation scheme based on the lattice-Boltzmann method to simulate the dynamics of charged colloids in an electrolyte. In our model we describe the electrostatics on the level of a Poisson-Boltzmann equation and the hydrodynamics of the fluid by the linearized Navier-Stokes equations. We verify our simulation scheme by means of a Chapman-Enskog expansion. Our method is applied to the calculation of the reduced sedimentation velocity U/U_0 for a cubic array of charged spheres in an electrolyte. We show that we recover the analytical solution first derived by Booth [F. Booth, J. Chem. Phys. **22**, 1956 (1954)] for a weakly charged, isolated sphere in an unbounded electrolyte. The present method makes it possible to go beyond the Booth theory, and we discuss the dependence of the sedimentation velocity on the charge of the spheres. Finally we compare our results to experimental data.

DOI: 10.1103/PhysRevE.64.061507 PACS number(s): 83.85.Pt, 47.65.+a, 47.11.+j, 05.20.Dd

I. INTRODUCTION

The simulation of the dynamics of colloidal suspensions is a challenging task. The reason is that the movement of the colloidal particles can be on a time scale that is orders of magnitudes slower than that of the solvent particles (e.g., seconds versus picoseconds). Therefore, simulation methods such as molecular dynamics, that account for the fluid particles explicitly, are not well suited to study the dynamics of colloidal suspensions because one would spend most of the simulation time solving the equations of motion of the fluid particles. The situation for charged colloids is even worse because one has to take into account the long-ranged Coulomb interactions that are already very time consuming in simple ionic liquids.

One possibility to circumvent these problems is to avoid explicit simulation of the solvent particles and describing the interaction between the colloidal particles by means of an effective potential. In the case of charged colloidal systems this is usually a Yukawa-like potential that gives in many cases quite an accurate description of interaction-dependent properties [1,2]. But the approach with effective interactions neglects completely the hydrodynamic interactions between the colloidal particles that stem from the momentum transport through the solvent. In order to take this into account one has to treat the hydrodynamics of the solvent at least on a coarse-grained level. An effective scheme that was developed to solve efficiently the Navier-Stokes equations, is the so-called lattice-Boltzmann method (LBM). The LBM is a preaveraged version of a lattice gas, i.e., a Boltzmann equation is solved on a lattice such that the Navier-Stokes equations are recovered (reviews of the method are the Refs. [3–5]). Recently, the LBM was applied to simulate the dynamics of colloidal systems, such as the rotational and translational short-time dynamics of colloids [6–10], the diffusion of colloidal particles in confined geometry [11–13], and the dynamics in porous media [14–17]. Also other complex systems such as polymer solutions [18] have been investigated by LBM.

Several attempts to apply the LBM to charged systems have been reported in the literature. He and Li [19] proposed a scheme that is appropriate to study electrochemical processes in an electrolyte. However, in this method it is assumed that the fluid is *locally* electrically neutral that cannot be true for the part of an electrolyte forming the electrical double layer around a macroion. Thus, the LBM of He and Li cannot be used to describe the dynamics of suspensions of charged colloids. A different LBM for charged systems was suggested by Warren [20]. The central idea of this method is the introduction of external charge densities ρ_s for the ionic species of type s that are propagated with the one-particle distribution function of the LB equation by means of the so-called moment propagation method [21]. These ionic densities are coupled back to the mass current of the LB equation via a chemical potential that consists of a term proportional to $\ln \rho_s$ and a term proportional to the electrostatic potential such that it only gives a contribution if the ion densities are not distributed as expected in equilibrium by a Boltzmann distribution (e.g., because of an external electrical field). Finally, the electrostatic potential is determined from the charge densities by means of a Poisson equation solver. The main drawback of Warren's method is that the charge densities are introduced as additional physical quantities that are independent from the mass density in the LB equation, and thus, this method is not self-consistent and the correctness of coupling of the charge density to the mass current is not obvious.

Our LBM for charged colloidal suspensions is inspired by Warren's approach, but it does not introduce ionic species as additional quantities. The details of our method can be found in the following sections. We apply it to the determination of the sedimentation velocity of an array of charged spheres in an electrolyte.

The paper is organized as follows. In Sec. II we give a brief introduction into the electrokinetic equations of motion with which we model the dynamics of the fluid. In Sec. III the LBM is presented that solves the latter equations of motion on a lattice. The LBM is verified in Sec. IV by means of

*Author to whom correspondence should be addressed. Email address: horbach@amolf.nl

 ©2001 The American Physical Society

a Chapman-Enskog expansion. And in Sec. V we show our results for the sedimentation phenomena. We conclude with a discussion of the method and the results.

II. THE ELECTROKINETIC EQUATIONS

In this section we introduce the equations of motion for a hydrodynamic description of charged colloidal suspensions. These equations can be found in standard textbooks (see e.g., Ref. [22]).

Consider a system of macroions with radius a in an electrolyte consisting of two ionic species that have charges $+z_1e$ and $-z_2e$, respectively, where z_1 and z_2 are the valencies of the ions and e is the charge of a proton. The densities of the ions, $\rho_1(\vec{r},t)$ and $\rho_2(\vec{r},t)$, are conserved quantities and therefore each of them follows a continuity equation

$$\frac{\partial \rho_s}{\partial t} = -\nabla \cdot \vec{J}_s \quad s=1,2. \tag{1}$$

The current $\vec{J}_s$ is given by

$$\vec{J}_s = \rho_s \vec{u} - D_s \nabla \rho_s - z_s D_s \rho_s \nabla \hat{\Phi}. \tag{2}$$

The first term in Eq. (2) in which $\vec{u}$ denotes the flow velocity is the convection current whereas the two other terms describe the diffusive current and the current due to the electrostatic potential Φ. D_s denotes the diffusivity of ions of type s and $\hat{\Phi}$ is the electrostatic potential in dimensionless form, $\hat{\Phi}=[e/(k_BT)]\Phi$, where k_B is Boltzmann constant and T is temperature.

$\hat{\Phi}$ is determined by the Poisson equation,

$$\nabla^2 \hat{\Phi} = -4\pi l_B \left(\sum_{s=1}^{2} z_s \rho_s + \sigma \right), \tag{3}$$

where the Bjerrum length l_B is defined by

$$l_B = \frac{e^2}{4\pi \epsilon k_B T}, \tag{4}$$

and ϵ is the dielectric constant. At a distance l_B the Coulomb energy of one ion due to another ion is equal to k_BT. σ denotes the charge density of the macroion. We assume that the charge Z of each macroion sits on its surface in the form of uniformly distributed point charges.

If we set $\vec{u}=0$ in Eqs. (1) and (2) we yield the equilibrium solution for the ion densities as

$$\rho_s(\vec{r}) = \overline{\rho_s} \exp(-z_s \hat{\Phi}(\vec{r})). \tag{5}$$

By putting the Boltzmann distribution (5) into the Poisson equation (3) this leads to the so-called Poisson-Boltzmann equation in which correlations between the ions are neglected. Moreover, if one linearizes the exponential function in Eq. (5) (Debye-Hückel theory) it is possible to solve Eq. (3) analytically and the result is a Yukawa potential,

$$\hat{\Phi}(\vec{r}) = K \frac{\exp(-|\vec{r}|/\lambda_D)}{|\vec{r}|}. \tag{6}$$

The so-called Debye length is defined by

$$\lambda_D \equiv \kappa^{-1} = \frac{1}{\sqrt{4\pi l_B \sum_s z_s^2 \overline{\rho_s}}}. \tag{7}$$

The potential (6) is even a good approximation in the nonlinear case but the prefactor K is then different from the one of the linear theory.

The equation of motion that has to be specified finally is that for the total mass current of the fluid, $\rho\vec{u} \equiv (\Sigma_{s=1}^2 \rho_s + \rho_n)\vec{u}$, where ρ_n is the density of the neutral part of the fluid. We assume that our fluid can be described by the linearized Navier-Stokes equations for low Reynolds number flow. Hence, the equation for $\rho\vec{u}$ with a body force due to the electrostatic potential is

$$\frac{\partial(\rho\vec{u})}{\partial t} = \nu \nabla^2 \rho \vec{u} - \nabla p - k_B T \sum_s z_s \rho_s \nabla \hat{\Phi}, \tag{8}$$

where p is the pressure and ν is the kinematic viscosity. If the equation for the pressure is the one of an ideal gas, $p=k_BT\rho$, p can be decomposed into an electrostatic and a neutral part, $p_e=k_BT\Sigma_{s=1}^2\rho_s$ and $p_n=k_BT\rho_n$, respectively. The sum of $-\nabla p_e$ and the electrostatic body force, i.e., the last term in Eq. (8), is zero, if the ion densities have relaxed to their equilibrium distribution, Eq. (5).

III. THE LATTICE-BOLTZMANN METHOD FOR CHARGED COLLOIDS

We have developed a simulation method to solve the nonlinear coupled Eqs. (1), (3), and (8) numerically. For this we use concepts that are well known from the LBM.

In this method the discretized version of a Boltzmann equation is solved numerically on a lattice on which every lattice point represents a cell of particles. The central quantity is the one-particle distribution function $n_i(\vec{r},t)$ that describes the number of particles on a lattice node $\vec{r}$ at time t with a discrete velocity $\vec{c}_i$. The discrete space of velocities $\{\vec{c}_i\}$ is chosen such that no artificial anisotropic terms appear in the corresponding equations in the continuous limit. In our case the velocity space consists of 18 vectors of which, from a given lattice node, six point to the nearest and 12 to next-nearest neighbors on a simple cubic lattice. This velocity space can be constructed by projecting the unit vectors of a four dimensional FCHC lattice onto three dimensions. It is one possible choice of a velocity space that exhibits the required isotropy.

The equation of motion for $n_i(\vec{r},t)$ consists of two steps, a collision and a propagation step. In the collision step the interaction between the particles is taken into account that results in the postcollision function $n_i^\star(\vec{r},t^\star)$ at the collision

time $t^\star$. In the propagation step $n_i(\vec{r},t)$ is updated by

$$n_i(\vec{r}+\vec{c}_i,t+1)=n_i^\star(\vec{r},t^\star). \tag{9}$$

In this equation the lattice constant, the time step, and the mass of a particle is set to unity. The density $\rho(\vec{r},t)$ and the mass current $\vec{j}\equiv\rho\vec{u}$ are given by the zeroth and first moment of n_i, respectively, $\rho=\Sigma_i n_i(\vec{r},t)$, $\vec{j}=\Sigma_i n_i(\vec{r},t)\vec{c}_i$.

In the case of the charged system a one-particle distribution function for each ion species and a neutral part is required. The purpose of the neutral part is to keep the viscosity essentially constant through the fluid. Thus, it is chosen such that its value at a given lattice point is much higher than that of the ionic densities. We make the following ansatz for the postcollision function $n_i^{s\star}$ for the counterions and coions, $s=+,-$, respectively, and the neutral part, $s=n$ (we also take into account rest particles by the index $i=0$),

$$n_i^{s\star}(\vec{r},t^\star)=\frac{\mathrm{w}_i\gamma_s}{24}\rho_s(\vec{r},t)\left(1+\frac{1}{c_{\mathrm{sv}}^2\rho'(\vec{r},t)}\vec{j}(\vec{r},t)\cdot\vec{c}_i\right), \tag{10}$$

$$n_0^{s\star}(\vec{r},t^\star)=(1-\gamma_s)\rho_s(\vec{r},t). \tag{11}$$

The factor w_i is a weighting factor that is equal to 2 for the $\vec{c}_i$ in the direction of nearest neighbors and equal to 1 for the remaining $\vec{c}_i$. So it satisfies the normalization constraint $\Sigma_{i=1}^{18}\mathrm{w}_i/24=1$. For the following we define also $\mathrm{w}_0=0$. With the parameter $0<\gamma_s\leqslant 1$ the diffusivity D_s of the particles of type s can be varied. The latter quantity is given by

$$D_s=\frac{c_{\mathrm{sv}}^2}{2}\gamma_s, \tag{12}$$

which is shown in the next section. c_{sv} is the sound velocity that is $1/\sqrt{2}$ for our model [4]. The density ρ' is defined by $\rho'=\Sigma_s\gamma_s\rho_s$.

The propagation step for our charged system is

$$n_i^s(\vec{r}+\vec{c}_i,t+1)=n_i^{s\star}(\vec{r},t^\star), \tag{13}$$

$$n_0^s(\vec{r},t+1)=n_0^{s\star}(\vec{r},t^\star). \tag{14}$$

Different propagation rules have to be established at the surface of the macroions and at the walls. Here we use the bounce back rules suggested by Ladd [4] that lead to no-slip boundary conditions. In this scheme one puts a sphere that represents a macroion onto the lattice whereby its surface cuts links between lattice nodes. The boundary nodes are defined halfway along these links and the population functions n_i^s that point to the direction of the boundary nodes are reflected back during the propagation step. In the case of moving boundaries there is a momentum transfer between the boundary nodes and the fluid. In this case the self-consistent scheme derived by Lowe *et al.* [9] and Heemels *et al.* [10] can be used.

The aforementioned way of mapping a sphere onto the lattice introduces fluid inside and outside the sphere. In our scheme we assign the charge of the macroions in that the inner fluid is an electrolyte with net charge Z. Charge neutrality requires that the total charge of the outer fluid equals the one of the inner fluid of the macroions. Of course, it is not allowed in our scheme that outer fluid leaks through the surface of the sphere. Therefore, only small movements of a macroion are possible such that the center of mass of the sphere can be fixed, and only a momentum transfer with the fluid takes place.

The densities ρ_s and the total mass current $\vec{j}$ cannot be inferred simply from the zeroth and first moments of the n_i^s's because we have to take into account their coupling to the gradient of the electrostatic potential. If ρ_s and $\vec{j}$ are calculated as

$$\rho_s(\vec{r},t+1)=\sum_{i=0}^{18}\left[n_i^s(\vec{r},t+1)-\frac{z_s}{2}\frac{\mathrm{w}_i\gamma_s}{24}\rho_s(\vec{r}-\vec{c}_i,t)\nabla\hat{\Phi}(\vec{r}-\vec{c}_i,t)\cdot\vec{c}_i\right] \tag{15}$$

and

$$\vec{j}(\vec{r},t+1)=\sum_{s=1}^{3}\left[\sum_{i=1}^{18}n_i^s(\vec{r},t+1)\vec{c}_i-c_{\mathrm{sv}}^2 z_s\gamma_s\rho_s(\vec{r},t+1)\nabla\hat{\Phi}(\vec{r},t+1)\right], \tag{16}$$

we are consistent with Eqs. (1) and (8) in the continuous limit. $\nabla\hat{\Phi}$ does not couple to the neutral part of the fluid. This is guaranteed in Eqs. (15) and (16) by setting $z_s=0$ for $s=n$.

If one replaces $n_i^s(\vec{r},t+1)$ by $n_i^s(\vec{r}-\vec{c}_i,t)$ in Eqs. (15) and (16) by using Eq. (13) it becomes clear that Eqs. (15) and (16) are the discrete versions of Eqs. (1) and (8), respectively. Thereby, the second terms in Eqs. (15) and (16) correspond, respectively, to the current due to the electrostatic potential in Eq. (1) and the electrostatic body force in Eq. (8). We show this explicitly in the next section by means of a Chapman-Enskog expansion. Of course, with the $\nabla\hat{\Phi}$ terms in Eqs. (15) and (16) the conservation of the ionic densities and the mass current is still fulfilled. This is guaranteed because $\hat{\Phi}$ is determined self-consistently from the ionic densities by means of the Poisson equation.

This means that we have to solve the Poisson equation at each time step in order to determine the electrostatic potential from the ionic densities ρ_+ and ρ_-. For this purpose we use a successive over-relaxation (SOR) scheme in which one looks in principle for the stationary solution of a diffusion equation [23]. But in contrast to a normal diffusion equation one introduces an acceleration parameter $1<\omega<2$ such that the potential is obtained as the iterative solution of the following equation:

$$\hat{\Phi}_{h+1}(\vec{r},t)=\omega\Bigg[\sum_i \Bigg(\frac{w_i}{24}\hat{\Phi}_h(\vec{r}-\vec{c}_i,t) + 4\pi l_B \frac{c_{sv}^2}{2}\sum_{s=+,-} z_s\rho_s(\vec{r},t)\Bigg)\Bigg] + (1-\omega)\hat{\Phi}_h(\vec{r},t). \quad (17)$$

In this equation we have denoted the iteration time by h (the unit for an iteration step is again set to unity). For a sufficient number of iteration steps Φ_h converges to Φ. We have found that a suitable choice for ω is 1.45 that guarantees stability and optimal acceleration. The gradient of $\hat{\Phi}$ that we need in Eqs. (15) and (16) is given by

$$\nabla\hat{\Phi}(\vec{r})=-\sum_i \frac{w_i}{24c_{sv}^2}\hat{\Phi}(\vec{r}-\vec{c}_i)\vec{c}_i. \quad (18)$$

Note that we use in Eqs. (17) and (18) the same discrete space as the velocity space in the lattice-Boltzmann equations. This means that the truncation error that is caused due to the discrete representation of the derivatives is of fourth order in contrast to a second order truncation error on a simple cubic lattice with six vectors $\{\vec{c}_i\}$ pointing to the nearest neighbors from a given lattice node. The stability and efficiency of the SOR algorithm are further optimized by making use of a partially decoupled red-black Gauss-Seidel scheme [24].

IV. CHAPMAN-ENSKOG EXPANSION

By means of a Chapman-Enskog expansion we show in this section that the set of discrete equations from the preceding section indeed recover the Eqs. (1), (3), and (8) in the continuous limit.

As a first step we rewrite Eqs. (15) and (16) for the densities ρ_s and the partial currents $\vec{j}_s\equiv\gamma_s\rho_s\vec{j}/\rho'$,

$$\rho_s(\vec{r},t)=\sum_i \frac{w_i\gamma_s}{24}\Bigg[\rho_s(\vec{r}-\vec{c}_i,t-1)+\vec{j}_s(\vec{r}-\vec{c}_i,t-1)\cdot\vec{c}_i + \frac{z_s}{2}\rho_s(\vec{r}-\vec{c}_i,t-1)\nabla\hat{\Phi}(\vec{r}-\vec{c}_i,t-1)\cdot\vec{c}_i\Bigg], \quad (19)$$

$$\vec{j}_s(\vec{r},t)=\sum_i \frac{w_i\gamma_s}{24}[\rho_s(\vec{r}-\vec{c}_i,t-1)\vec{c}_i+\vec{j}_s(\vec{r}-\vec{c}_i,t-1)\cdot\vec{c}_i\vec{c}_i] - c_{sv}^2\gamma_s z_s\rho_s(\vec{r},t)\nabla\hat{\Phi}(\vec{r},t). \quad (20)$$

If we now expand the functions of the form $f(\vec{r}-\vec{c}_i,t-1)$ $(f=\rho_s,\vec{j}_s,\rho_s\nabla\hat{\Phi})$ around position $\vec{r}$ and time t up to second order,

$$f(\vec{r}-\vec{c}_i,t-1)=f(\vec{r},t)+\Bigg[-\partial_t-c_{i\alpha}\nabla_\alpha+\frac{1}{2}(\partial_t+c_{i\alpha}\nabla_\alpha)^2\Bigg]f(\vec{r},t), \quad (21)$$

we obtain the following equations for ρ_s and $\vec{j}_s$:

$$\partial_t\rho_s=\frac{1}{2}\partial_t^2\rho_s-\nabla\cdot\vec{j}_s+\partial_t\nabla\cdot\vec{j}_s+\frac{c_{sv}^2}{2}\gamma_s(\nabla^2\rho_s+z_s\nabla\cdot\rho_s\nabla\hat{\Phi} + z_s\partial_t\nabla\cdot\rho_s\nabla\hat{\Phi}), \quad (22)$$

$$\partial_t\vec{j}_s=-c_{sv}^2\gamma_s\nabla\rho_s+c_{sv}^2\gamma_s\partial_t\nabla\rho_s+\frac{1}{2}\partial_t^2\vec{j}_s+\frac{1}{6}\nabla^2\vec{j}_s - c_{sv}^2\gamma_s z_s\rho_s\nabla\hat{\Phi}. \quad (23)$$

To achieve Eqs. (22) and (23) we have used the lattice sums [4]

$$\sum_{i=1}^{18} c_{i\alpha}c_{i\beta}=c_{sv}^2\delta_{\alpha\beta}, \quad (24)$$

$$\sum_{i=1}^{18} c_{i\alpha}c_{i\beta}c_{i\gamma}c_{i\delta}=\frac{1}{3}(\delta_{\alpha\beta}\delta_{\gamma\delta}+\delta_{\alpha\gamma}\delta_{\beta\delta}+\delta_{\alpha\delta}\delta_{\beta\gamma}). \quad (25)$$

Equations (22) and (23) are the starting point for the Chapman-Enskog expansion that introduces a macroscopic space scale by $\vec{r}_1=\epsilon\vec{r}$ and two macroscopic time scales by $t_1=\epsilon t$ and $t_2=\epsilon^2 t$. The t_1 scale describes fast convection processes whereas on the slower t_2 scale the diffusion of vorticity takes place. Thus, the Chapman-Enskog expansion enables us to consider the latter time scales separately. It was for the first time applied to lattice gases by Frisch *et al.* [25].

We now express the derivatives by means of $\vec{r}_1$, t_1, and t_2,

$$\nabla=\epsilon\nabla_1, \quad (26)$$

$$\partial_t=\epsilon\partial_{t_1}+\epsilon^2\partial_{t_2}, \quad (27)$$

and put them into Eqs. (22) and (23). If we collect terms of the same order in ϵ we obtain on the ϵ^1 scale

$$\partial_{t_1}\rho_s=-\nabla_1\cdot\vec{j}_s, \quad (28)$$

$$\partial_{t_1}\vec{j}_s=-c_{sv}^2\gamma_s(\nabla_1\rho_s+z_s\rho_s\nabla_1\hat{\Phi}). \quad (29)$$

Equation (28) is the continuity equation for mass conservation. If one takes the sum over s on both sides of Eq. (29) one obtains the ''fast'' part of the linearized Navier-Stokes equation for the total mass current $\vec{j}$

$$\partial_{t_1}\vec{j}=-c_{sv}^2\sum_s(\nabla\rho_s+z_s\rho_s\nabla_1\hat{\Phi}). \quad (30)$$

The first term on the right-hand side of this equation is the negative gradient of the pressure and the second term the electrostatic body force.

On the ϵ^2 scale we have

$$\partial_{t_2}\rho_s=\frac{1}{2}\partial_{t_1}^2\rho_s+\partial_{t_1}\nabla_1\cdot\vec{j}_s+\frac{c_{sv}^2}{2}\gamma_s(\nabla_1^2\rho_s+z_s\nabla_1\rho_s\nabla\hat{\Phi}), \tag{31}$$

$$\partial_{t_2}\vec{j}_s=c_{sv}^2\gamma_s\partial_{t_1}\nabla_1\rho_s+\frac{1}{2}\partial_{t_1}^2\vec{j}_s+\frac{1}{6}\nabla^2\vec{j}_s. \tag{32}$$

From Eqs. (28)–(32) we see that the transport of the ion densities to equilibrium can be either achieved by convection or by diffusion. So, if $\partial_{t_1}\vec{j}_s$ vanishes Eq. (29) is solved by the Boltzmann distribution, Eq. (5). And by using Eqs. (28) and (29), Eq. (31) for the densities simplifies to

$$\partial_{t_2}\rho_s=0. \tag{33}$$

This equation implies that the fluid is incompressible on the t_2 scale. In this case there is no diffusion on the t_2 scale because the ionic densities have already come to their equilibrium on the faster t_1 scale. On the other hand, if we assume that the second derivative of ρ_s with respect to t_1 vanishes then Eq. (31) becomes a diffusion equation with the diffusion constant $D_s=c_{sv}^2\gamma_s/2$ for ions of type s. The diffusion process relaxes the densities ρ_s $(s=+,-)$ again to the equilibrium distribution (5).

We still have to discuss Eq. (32) for the mass current on the t_2 scale. It is reasonable to assume that the derivatives of ρ_s and $\vec{j}_s$ with respect to t_1 are small on the t_2 scale. So we may neglect the first two terms in Eq. (32). Furthermore, we have to sum over s on both sides of Eq. (32) in order to obtain the equation of motion for the total current $\vec{j}$ on the t_2 scale

$$\partial_{t_2}\vec{j}=\frac{1}{6}\nabla_1^2\vec{j}. \tag{34}$$

Moreover, if we combine this equation with Eq. (29) for variations on the t_1 scale we obtain the following equation:

$$\partial_t\vec{j}=\frac{1}{6}\nabla^2\vec{j}-c_{sv}^2\sum_s\ \gamma_s\nabla\rho_s-c_{sv}^2\sum_s\ \gamma_s z_s\rho_s\nabla\hat{\Phi}. \tag{35}$$

So, we recover Eq. (8) for the total current whereby the kinematic viscosity ν is one-sixth and the equation for the pressure depends on the parameters γ_s,

$$p=c_{sv}^2\sum_s\ \gamma_s\rho_s. \tag{36}$$

Note that for $\gamma_1=\gamma_2$ this is just the equation of state for an ideal gas.

V. THE SEDIMENTATION VELOCITY

In this section we present the results for the sedimentation velocity of an array of charged spheres in an electrolyte solution. We show that our method gives correct results in that it recovers an analytical formula that is valid in the limit of an isolated, weakly charged sphere in an unbounded electrolyte. Furthermore, we discuss the dependence of the sedimentation velocity on the charge of the spheres. We then compare our results to experimental data.

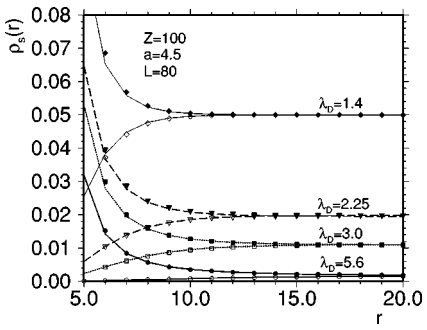

FIG. 1. The radial ionic densities around a macroion with $a=4.5$ for $Z=100$ as determined directly from $\rho_s(\vec{r})$ (filled symbols for the counterions and open symbols for the coions) and by calculating it from the electrostatic potential (lines); see text, for the indicated Debye lengths λ_D.

Before we show the results for the sedimentation velocity we discuss to what extent the calculated electrostatic potentials and the ionic densities around a macroion are influenced by lattice artifacts. The latter may have several reasons. We use a simple way to introduce the charge of a macroion. We assign its charge Z by distributing the densities on the lattice nodes inside the macroion such that the net charge, i.e., the sum over all these nodes, is equal to Z. This may have the effect that the effective charge distribution on the surface of the macroion is anisotropic because the inner nodes form only an approximative representation of a sphere that can, of course, be improved by increasing its radius a. Another drawback that is due to the lattice lies in the range of the electrostatic potential. The Debye length, measured in lattice units, must be at least larger than one. Otherwise, the simulation becomes unstable because one has strong discontinuities in the ionic densities between two lattice points close to the surface of the macroion.

The importance of these artifacts can be checked by determining the radial ionic densities $\rho_s(r)$ around a spherical macroion, i.e., the densities for the ions of type s at a distance r from the center of the sphere. In the absence of artifacts $\rho_s(r)$ should obey

$$\rho_s(r)=\overline{\rho}_s\exp(-z_s\hat{\Phi}(r)). \tag{37}$$

In Fig. 1 we show an example of the $\rho_s(r)$ calculated directly (symbols) and from the right-hand side of Eq. (37) (solid lines) for a macroion with a radius $a=4.5$ and charge $Z=100$. The length of the simulation box is $L=80$ and the density of the neutral fluid is set to $\rho_n=20$. The Debye length is varied by changing the sum of the mean ionic densities from $\Sigma_s\overline{\rho}_s=0.0063$ $(\lambda_D=5.6)$ to $\Sigma_s\overline{\rho}_s=0.1$ $(\lambda_D=1.4)$ whereby the Bjerrum length is $l_B=0.4$. We can infer from Fig. 1 that the ionic densities as calculated directly agree very well with those calculated from the right-hand side of Eq. (37) even for a Debye length as small as λ_D

$=1.4$. This means that $a=4.5$ is a reasonable choice for the radius of a macroion that keeps lattice artifacts small at least for $\lambda_D \geqslant 1.4$.

Now we consider one charged macrosphere in a unit cell of length L with a fixed position. It represents one particle in an array of spheres on a simple cubic lattice because it interacts with its own periodic images. The volume fraction of the macroions is given by $\varphi=(4\pi a^3)/(3L^3)$. In order to investigate sedimentation phenomena we have to introduce a gravitational force in the LB equations. After a time of the order $\tau_s=L^2/\nu_{\rm eff}$ ($\nu_{\rm eff}$ is effective, kinematic viscosity of the fluid in the presence of the spheres) the steady state is reached for which one determines the average flow velocity in the unit cell. We divide the latter by the average flow velocity of the corresponding neutral system and yield the ratio U/U_0 of the sedimentation velocities in the charged and the neutral system, respectively. For the larger systems considered, we did not wait until the system came to its steady state, because we know that the time dependence of the apparent sedimentation velocity $U_{\rm app}(t)$ is given by

$$U_{\rm app}(t)=U\left[1-\exp\left(-\frac{t}{\tau_s}\right)\right]. \tag{38}$$

By computing numerically the time derivative of Eq. (38) one obtains a simple exponential function with the two unknown quantities U and τ_s that we computed from fits of the logarithm of this exponential function. With this procedure it was possible to determine U within a time of the order $t \approx \tau_s/20$. We checked the accuracy of our fits at $\varphi=0.0018$ by comparing them to the exact steady state results, and we obtained identical results for U/U_0 as a function of κa ($\kappa \equiv \lambda_D^{-1}$).

In the following we show that our LB method recovers an analytical result for U/U_0 which was first derived by Booth [26], and later slightly modified by Ohshima *et al.* [27].[1] It is valid in the limit of infinite dilution and small charge of the macroions, i.e., a weakly charged macroion in an electrolyte with infinite extension. What do we expect in this case? Due to the external force the ionic concentrations around the macroions that form the electrical double layer deviate from their equilibrium values. The double layer loses its spherical symmetry due to the fluid motion that results in an electrical dipole field pointing in the direction opposite to the motion of the macroion and thus reduces its sedimentation velocity. Booth's calculation starts with the ansatz

$$\frac{U}{U_0}=1+\sum_{k=1}^{\infty} c_k Z^k \tag{39}$$

and takes into account only terms in the lowest nonvanishing order in Z^k,

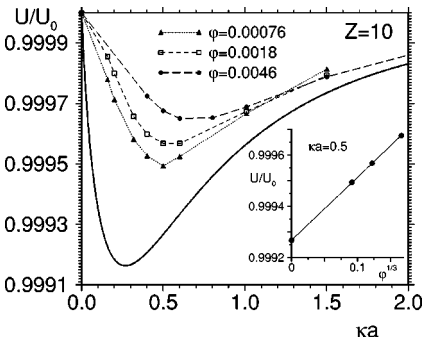

FIG. 2. U/U_0 for the volume fractions $\varphi=0.0046$, 0.0018, and 0.000 76 as a function of κa. The charge of the macroion is set to $Z=10$. The solid line is the result from Booth's theory. The inset shows U/U_0 as a function of $\varphi^{1/3}$ for $\kappa a=0.5$. The solid line in the inset is the fit function $0.999\,269+0.002\,455\,6\varphi^{1/3}$.

$$\frac{U}{U_0}=1+c_2 Z^2. \tag{40}$$

The coefficient c_2 can be calculated analytically by solving the electrokinetic equations of motion (1), (3), and (8) whereby the Poisson equation is solved in the Debye-Hückel limit. The final expression for c_2 has the following form [26,27],

$$c_2=-\frac{k_B T l_B}{72\pi a^2 \eta}\frac{\sum_s z_s^4 \overline{\rho_s} D_s^{-1}}{\sum_s z_s^2 \overline{\rho_s}} f(\kappa a), \tag{41}$$

where $\overline{\rho_s}$ denotes the mean density of the ions of type s far away from the center of the macroion, η is the shear viscosity, $f(\kappa a)$ is a function of exponential integrals of different order n, $E_n(x)=x^{n-1}\int_x^\infty dt\, t^{-n}\exp(-t)$.

$$\begin{aligned} f(\kappa a)=\frac{1}{1+(\kappa a)^2}\{&e^{2\kappa a}[3E_4(\kappa a)-5E_6(\kappa a)]^2 \\ &+8e^{\kappa a}[E_3(\kappa a)-E_5(\kappa a)]-e^{2\kappa a}[4E_3(2\kappa a) \\ &+3E_4(2\kappa a)-7E_8(2\kappa a)]\}. \end{aligned} \tag{42}$$

We have determined U/U_0 as a function of κa for different volume fractions. The radius of the macroion is fixed to $a=4.5$. Moreover, the diffusivities of the ionic species in the fluid are chosen to be $D_1=0.165$ for the counterions and $D_2=0.25$ for the coions. The ratio $D_1/D_2=0.66$ corresponds to that of $D_{\rm Na}/D_{\rm Cl}$ in sodium chloride. The Bjerrum length is again set to $l_B=0.4$. In order to vary κa from 0.15 to 1.5 we have to change $\Sigma_s \overline{\rho_s}$ from 0.000 25 to 0.022 11, respectively. This is small compared to the density of the neutral fluid, $\rho_n=20$. So by changing κa we do not change the viscosity of the fluid significantly.

Figure 2 shows the results for a surface charge $Z=10$ of the macroion. We demonstrate below that this value is small enough for the approximation (28) to hold. First, we infer from Fig. 2 that the relative reduction of the sedimentation

[1]However, Booth's result agrees with the one of Ohshima *et al.* for an 1-1-electrolyte. We are only interested in this special case in this paper.

velocity due to the charges is only of the order of 10^{-4} at $Z=10$ in the φ range considered. U/U_0 exhibits a minimum that moves to higher values of κa with increasing φ. The occurrence of such a minimum is reasonable since an increase of κa is accompanied with two competing effects. On the one hand, the electrostatic potential $\hat{\Phi}$ becomes stronger due to an increasing salt concentration but, on the other hand, it becomes also more short ranged because of a decreasing Debye length, and thus, it affects only the flow near the macroion. The value of the minimum in U/U_0 decreases with decreasing φ and seems to move towards the one of the Booth curve for $\varphi \to 0$. This also holds for the amplitude and the shape of U/U_0 for $\varphi \to 0$. In order to give quantitative evidence that our calculation would recover Booth's result we plot in the inset of Fig. 2, U/U_0 as a function of $\varphi^{1/3}$ at $\kappa a=0.5$, i.e., around the position of the minimum. The fit in this figure with a straight line indeed approaches the Booth result, i.e., at $\varphi=0$.

Up to now we have shown only the results for U/U_0 for a small charge of the macroion $Z=10$. But it is of course interesting to check up to which values of Z the approximation (40) holds. If Eq. (40) would be exact, one could renormalize U/U_0 as a function of κa for a given charge $Z=Z_{\mathrm{old}}$ to a new charge $Z=Z_{\mathrm{new}}$ by multiplying $1-U/U_0$ by $Z_{\mathrm{new}}^2/Z_{\mathrm{old}}^2$. In this way we have renormalized our data for $Z=10$ at $\varphi=0.000\,76$ to $Z=100$ and $Z=130$, and we compare these data sets in Fig. 3(a) with the corresponding simulation results for the latter two values of Z. We see that we have strong corrections to the results as expected from Booth's theory, especially around the minimum in U/U_0. First the amplitude of the minimum is underestimated by the renormalized curves and also the position of the minimum is at a slightly larger value. To study the corrections to Booth's theory more quantitatively we plot in Fig. 3(b), $1-U/U_0$ as a function of Z for $\kappa a=0.16$,0.5, and 1.5. The solid lines in this figure are fits of the form $g(Z)=c_2Z^2+c_4Z^4+c_6Z^6$. From the comparison of the different functions $g(Z)$ to the corresponding ones with only the leading term proportional to Z^2 [dashed curves in Fig. 3(b)] we can conclude that the corrections to Booth's theory become important for $Z>50$.

Finally we address the question whether our results are in agreement with a dynamic light scattering experiment by Schumacher and van de Ven [28]. They measured the diffusion constant D for a system of gold particles in distilled water. Note that D/D_0 is equal to U/U_0. The radius of the gold particles was around 20 nm and their volume fraction $(2\times10^{-5})\%$. Different data sets were determined by changing the value of κa with different salts. We consider here the experimental data points measured with sodium chloride that are shown in Fig. 4 in comparison to our simulation data at $\varphi=0.0046$ and at $\varphi=0.000\,76$ for $Z=100$. It is interesting that the experimental data can be very well described by the simulation curve for $\varphi=0.0046$ although the experiment was done at a very small volume fraction of gold particles and the curve for $\varphi=0.000\,76$ deviates strongly from the experimental data. More systematic experiments, e.g., for different volume fractions, would be necessary to clarify this discrepancy.

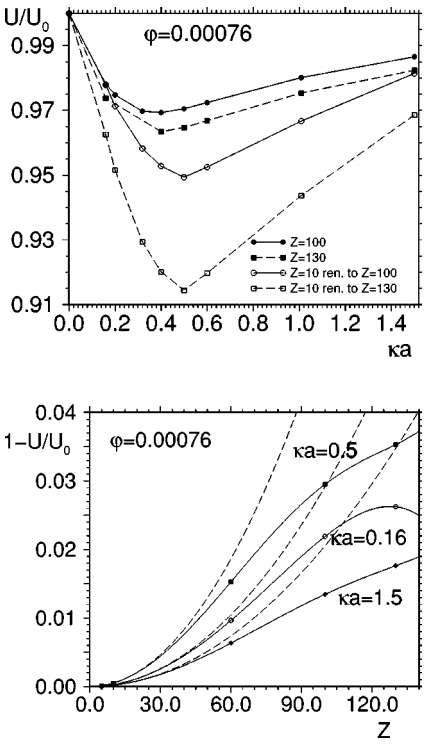

FIG. 3. (a) U/U_0 at $\varphi=0.000\,76$ as a function of κa for $Z=100$ and $Z=130$ (filled symbols). The open symbols show data for $Z=10$ that are renormalized to $Z=100$ and $Z=130$ (see text). (b) $1-U/U_0$ as a function of Z for the indicated values of κa. The solid lines show the following fit functions: $g(Z)=2.916\times10^{-6}Z^2-6.086\times10^{-11}Z^4-1.173\times10^{-15}Z^6$ for $\kappa a=0.16$, $g(Z)=5.182\times10^{-6}Z^2-2.810\times10^{-10}Z^4+5.801\times10^{-15}Z^6$ for $\kappa a=0.5$, $g(Z)=2.056\times10^{-6}Z^2-8.684\times10^{-11}Z^4+1.592\times10^{-15}Z^6$ for $\kappa a=1.5$. The dashed lines show only the term proportional to Z^2 of the latter three functions.

VI. CONCLUSIONS

We have developed a LBM for the simulation of the dynamics of suspensions of charged colloidal particles. In this method a set of nonlinear, coupled electrokinetic equations is solved that consists of convective diffusion equations for the ion densities ρ_s $(s=+,-)$, the linearized Navier-Stokes equations for the mass current $\vec{j}$, and the Poisson equation for the electrostatic potential $\hat{\Phi}$. Furthermore, a neutral fluid

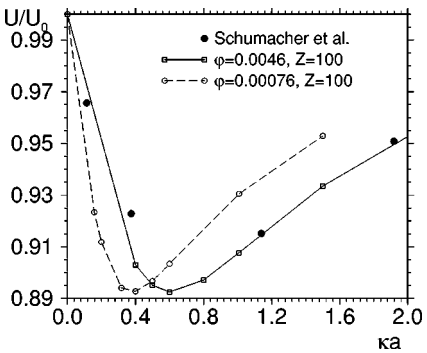

FIG. 4. U/U_0 at $\varphi=0.000\,76$ and $\varphi=0.0046$ as a function of κa for $Z=100$ in comparison to experimental data (closed circles).

characterized by the density ρ_n can be introduced in order to keep the viscosity in the fluid essentially constant. The propagation of ρ_s and $\vec{j}$ is computed by means of one-particle distribution functions n_i^s for each species s. But in contrast to the normal LBM ρ_s and $\vec{j}$ are not simply given as zeroth and first moments of the n_i^s's, respectively. This is due to the coupling of the ionic part of the fluid to the gradient of $\hat{\Phi}$ that leads to an additional diffusive term in the propagation of the ion densities and a body force term in the propagation of the mass current $\vec{j}$. The electrostatic potential is determined from the ion densities by means of a Poisson equation solver for which we use a successive over-relaxation scheme. Our method is fast, stable, and easy to implement. We have verified our numerical scheme by means of a Chapman-Enskog expansion.

As an application we applied our method to determine the reduced sedimentation velocity U/U_0 for an array of charged spheres on a simple cubic lattice. We determined U/U_0 as a function of the dimensionless parameter κa for different volume fractions of macroions φ. We compared our results with an analytical formula first derived by Booth that is valid in the limit of a weakly charged, isolated macroion in an unbounded electrolyte. Booth's theory starts with an expansion of U/U_0 in powers of the macroion charge Z of which the lowest nonvanishing order, Z^2 is taken into account. We gave evidence that we recover Booth's result in the limit $\varphi \to 0$. For about $Z > 50$, corrections to the Booth theory become important. Up to $Z = 130$ our simulation data can be well described by an expansion up to order Z^6. These numerical data could be used to test theories that go beyond the Booth level. We mention that very recently also a mode coupling theory with hydrodynamic interactions was shown to be in agreement with Booth's theory [29]. This theory is also able to consider colloidal systems at finite volume fractions.

Our LBM for charged colloids is well suited to study their short-time dynamics and the flow around macroions. It is not restricted to steady state problems but one can also determine time dependent quantities such as velocity autocorrelation function of a tagged macroion in a colloidal suspension. Also particle shapes, which are different from a spherical one can be easily introduced in our LBM. Moreover, the introduction of walls is rather simple, which makes it possible to study charged colloidal particles in confined geometries.

ACKNOWLEDGMENTS

We thank F. Capuani for a critical reading of the manuscript. The work of the FOM Institute is part of the scientific program of FOM and is supported by the Nederlandse Organisatie voor Wetenschappelijk Onderzoek (NWO). J.H. acknowledges financial support by the Deutsche Forschungsgemeinschaft (Grant No. HO 2231/1-1).

[1] M.J. Stevens, M.L. Falk, and M.O. Robbins, J. Chem. Phys. **104**, 5209 (1996).
[2] E. Allahyarov, H. Löwen, and S. Trigger, Phys. Rev. E **57**, 5818 (1998).
[3] R. Benzi, S. Succi, and M. Vergassola, Phys. Rep. **222**, 145 (1992).
[4] A.J.C. Ladd, J. Fluid Mech. **271**, 285 (1994); **271**, 311 (1994).
[5] S. Chen and G.D. Doolen, Annu. Rev. Fluid Mech. **30**, 329 (1998).
[6] A.J.C. Ladd, Phys. Rev. Lett. **70**, 1339 (1993).
[7] M.H.J. Hagen, D. Frenkel, and C.P. Lowe, J. Chem. Phys. **109**, 275 (1998).
[8] M.H.J. Hagen, D. Frenkel, and C.P. Lowe, Physica A **272**, 376 (1999).
[9] C.P. Lowe, D. Frenkel, and A.J. Masters, J. Chem. Phys. **103**, 1582 (1995).
[10] M.W. Heemels, M.H.J. Hagen, and C.P. Lowe, J. Comput. Phys. **164**, 48 (2000).
[11] M.H.J. Hagen, I. Pagonabarraga, C.P. Lowe, and D. Frenkel, Phys. Rev. Lett. **78**, 3785 (1997).
[12] I. Pagonabarraga, M.H.J. Hagen, C.P. Lowe, and D. Frenkel, Phys. Rev. E **58**, 7288 (1998).
[13] I. Pagonabarraga, M.H.J. Hagen, C.P. Lowe, and D. Frenkel, Phys. Rev. E **59**, 4458 (1999).
[14] U. Oxaal, E.G. Flekkoy, and J. Feder, Phys. Rev. Lett. **72**, 3514 (1994).
[15] A. Koponen, D. Kandhai, E. Hellen, M. Alava, A. Hoekstra, M. Kataja, K. Niskanen, P. Sloot, and J. Timonen, Phys. Rev. Lett. **80**, 716 (1998).
[16] C.P. Lowe and D. Frenkel, Phys. Rev. Lett. **77**, 4552 (1996).
[17] D.L. Koch, R.J. Hill, and A.S. Sangani, Phys. Fluids **10**, 3035 (1998).
[18] P. Ahlrichs and B. Dünweg, J. Chem. Phys. **111**, 8225 (1999).
[19] X. He and N. Li, Comput. Phys. Commun. **129**, 158 (2000).
[20] P.B. Warren, Int. J. Mod. Phys. C **8**, 889 (1997).
[21] D. Frenkel and M.H. Ernst, Phys. Rev. Lett. **63**, 2165 (1989).
[22] R. J. Hunter, *Foundations of Colloid Science* (Clarendon Press, Oxford, 1989), Vol. II.
[23] W. H. Press, S. A. Teukolsky, W. T. Vetterling, and B. P. Flannery, *Numerical Recipes* (Cambridge University Press, Cambridge, 1992).
[24] M.M. Gupta, J. Kouatchou, and J. Zhang, J. Comput. Phys. **132**, 226 (1997); J. Zhang, *ibid.* **143**, 449 (1998).
[25] U. Frisch, B. Hasslacher, and Y. Pomeau, Phys. Rev. Lett. **56**, 1505 (1986).
[26] F. Booth, J. Chem. Phys. **22**, 1956 (1954).
[27] H. Ohshima, T.W. Healy, L.R. White, and R.W. O'Brien, J. Chem. Soc., Faraday Trans. 2 **80**, 1299 (1984).
[28] G.A. Schumacher and T.G.M. van de Ven, Faraday Discuss. Chem. Soc. **83**, 75 (1987).
[29] M. Kollmann and G. Nägele, Europhys. Lett. **52**, 474 (2000); J. Chem. Phys. **113**, 7672 (2000).